

Radiative corrections to scalar masses and mixing in a scale invariant two Higgs doublet model

Jae Sik Lee^{1,2,3} and Apostolos Pilaftsis^{3,4}¹*Department of Physics, National Tsing Hua University, Hsinchu 300, Taiwan*²*Department of Physics, Chonnam National University, 300 Yongbong-dong, Buk-gu, Gwangju, 500-757, Republic of Korea*³*Consortium for Fundamental Physics, School of Physics and Astronomy, University of Manchester, Manchester M13 9PL, United Kingdom*⁴*Department of Theoretical Physics and IFIC, University of Valencia-CSIC, E-46100, Valencia, Spain*

(Received 9 April 2012; published 3 August 2012)

We study the Higgs boson mass spectrum of a classical scale invariant realization of the two Higgs doublet model (SI-2HDM). The classical scale symmetry of the theory is explicitly broken by quantum loop effects due to gauge interactions, Higgs self-couplings and top quark Yukawa couplings. We determine the allowed parameter space compatible with perturbative unitarity and electroweak precision data. Taking into account the LEP and the recent LHC exclusion limits on a standard-model-like Higgs boson HSM, we obtain rather strict constraints on the mass spectrum of the heavy Higgs sector of the SI-2HDM. In particular, if MHSM 125 GeV, the SI-2HDM strongly favors scenarios in which at least one of the nonstandard neutral Higgs bosons has a mass close to 400 GeV and is generically degenerate with the charged Higgs boson, whilst the third neutral Higgs scalar is lighter than 500 GeV.

DOI: [10.1103/PhysRevD.86.035004](https://doi.org/10.1103/PhysRevD.86.035004)

PACS numbers: 11.30.Ly, 11.30.Qc, 14.80.Ec, 14.80.Fd

I. INTRODUCTION

Classical scale symmetries provide a minimal and calculable approach to potentially solving the infamous gauge hierarchy problem. In the standard model (SM), the absence of the mass parameter m^2 from the Higgs potential renders the classical action of the theory scale invariant (SI). However, as originally discussed by Coleman and Weinberg [1] and later by Gildener and Weinberg [2], quantum loops generate logarithmic terms which anomalously break the scale invariance of the theory, giving rise to electroweak symmetry breaking. Given the LEP2 mass limit on the SM Higgs boson $M_{H_{SM}} > 114.4$ GeV [3] and the experimental value of the top quark mass $m_t \approx 173$ GeV, a perturbative SI version of the SM is not both theoretically and phenomenologically viable. In particular, the large top quark Yukawa coupling gives rise to an effective potential which is no longer bounded from below, at least at the perturbative level. This difficulty may be circumvented, if additional massive bosonic fields such as real and complex singlet scalars are present in SI extensions of the SM [4–10].

In this paper we study a minimal scale invariant two Higgs doublet model (SI-2HDM) extension of the SM. To naturally avoid flavor-changing neutral currents (FCNCs), we assume that the SI-2HDM potential is invariant under a Z_2 discrete symmetry [11], under which the two Higgs doublets $\Phi_{1,2}$ transform as $\Phi_{1(2)} \rightarrow +(-)\Phi_{1(2)}$. At the tree level, the spontaneous breaking of the classical scale symmetry due to the presence of a nonvanishing flat direction in the Higgs potential gives rise to a massless CP -even pseudo-Goldstone boson h . We calculate the radiative

corrections to the CP -even Higgs boson mass matrix that result from quantum loops of W^\pm and Z bosons, Higgs self-interactions and top quark Yukawa couplings. To determine the allowed parameter space of the SI-2HDM, we consider the theoretical constraints of convexity and perturbative unitarity, as well as phenomenological constraints from electroweak precision data and direct Higgs boson searches.

Taking all the aforementioned constraints into account, the allowed range of masses for the charged Higgs bosons H^\pm and the CP -odd scalar A gets significantly restricted. We find that for a 125-GeV SM-like Higgs boson H_1 , at least two Higgs states, charged (H^\pm) or neutral (H_2, A), are generically degenerate and have masses close to 400 GeV, whereas the third Higgs state has to be lighter than 500 GeV. In particular, there are three favorable scenarios with the above characteristics. In the first scenario, the CP -even Higgs boson H_2 and the CP -odd scalar A are almost degenerate with $M_{H_2} \sim M_A \sim 400$ GeV, and the charged Higgs boson H^\pm weighs between 295 GeV and 420 GeV, after taking into account the $b \rightarrow s\gamma$ constraint. The second favorable scenario contains a CP -odd state A lighter than 100 GeV, and the Higgs states H^\pm and H_2 have approximately equal masses $M_{H^\pm} \sim M_{H_2} \sim 400$ GeV. Finally, there is a third possibility, where the heavier CP -even Higgs boson H_2 can be lighter than 180 GeV, while the charged Higgs bosons H^\pm and the CP -odd scalar A are restricted to be almost degenerate, with $M_{H^\pm} \sim M_A \sim 400$ GeV.

The layout of the paper is as follows. After this brief introduction, in Sec. II we discuss in detail the Higgs sector of the SI-2HDM. Specifically, we first determine the flat

directions of the tree-level SI-2HDM potential and its scalar mass spectrum. We then calculate the one-loop effective potential of the SI-2HDM and evaluate the radiatively corrected masses of the CP -even Higgs bosons and their mixing. At the end of this section, we discuss the importance of the choice of the renormalization group (RG) scale in our analysis. In Sec. III we impose the theoretical constraint of perturbative unitarity and require compatibility of the theory against electroweak precision data and direct Higgs boson searches. In the light of these restrictions, we determine the allowed parameter space for the heavy Higgs sector of the SI-2HDM. Finally, Sec. IV summarizes our conclusions and discusses possible future directions.

II. SCALE INVARIANT TWO HIGGS DOUBLET MODEL

The 2HDM exhibits an exact classical scaling symmetry, if there are no explicit mass parameters in the scalar potential. To be specific, under global scale transformations

$$\varphi(x) \rightarrow \varphi'(x') = e^{d_\varphi \sigma} \varphi(e^\sigma x), \quad (1)$$

where σ is a constant, the action of the 2HDM Lagrangian $S[\varphi(x)]$ remains invariant; i.e., $S[\varphi(x)] = S[\varphi'(x')]$, where φ represents a generic bosonic (fermionic) field of the 2HDM, and $d_\varphi = 1$ ($3/2$) is its classical scaling dimension. Beyond the tree level, the classical scale invariance of the theory is broken by scalar operators of dimension $n > 4$, e.g. $\varphi^4 \ln(\varphi^2/\langle \varphi \rangle^2)$ with $d_\varphi = 1$, in a SI (or no-scale) regularization scheme, such as the scheme of dimensional regularization (see also [9], and references therein). This is the scheme that we consider here for performing our quantum loop calculations. Nevertheless, had we chosen a scheme with explicit UV cutoff dependence, we would have obtained the same results by demanding that the renormalized Coleman-Weinberg effective potential V_{eff} satisfy the conditions $d^n V_{\text{eff}}(\varphi)/d\varphi^n = 0$ at $\varphi = 0$, for $n = 0, 1, 2, 3$.

We note that our approach to formulating a classical SI theory differs from the one studied in [12,13], where the scale symmetry is imposed at the quantum level. As argued in [14], however, quantum SI theories face difficulties with renormalizability at high orders, and they can therefore be regarded only as effective field theories.

In this Section, after introducing the tree-level SI-2HDM potential, we determine its flat directions and the resulting scalar mass spectrum. Then, we calculate the one-loop effective potential, from which we derive the radiatively corrected Higgs boson masses. Finally, we comment on the choice of the RG scale.

A. Flat directions of the tree-level potential

At the tree level, the most general SI-2HDM potential reads

$$\begin{aligned} V^0 = & \lambda_1(\Phi_1^\dagger \Phi_1)^2 + \lambda_2(\Phi_2^\dagger \Phi_2)^2 + \lambda_3(\Phi_1^\dagger \Phi_1)(\Phi_2^\dagger \Phi_2) \\ & + \lambda_4(\Phi_1^\dagger \Phi_2)(\Phi_2^\dagger \Phi_1) + \frac{\lambda_5}{2}(\Phi_1^\dagger \Phi_2)^2 + \frac{\lambda_5^*}{2}(\Phi_2^\dagger \Phi_1)^2 \\ & + \lambda_6(\Phi_1^\dagger \Phi_1)(\Phi_1^\dagger \Phi_2) + \lambda_6^*(\Phi_1^\dagger \Phi_1)(\Phi_2^\dagger \Phi_1) \\ & + \lambda_7(\Phi_2^\dagger \Phi_2)(\Phi_1^\dagger \Phi_2) + \lambda_7^*(\Phi_2^\dagger \Phi_2)(\Phi_2^\dagger \Phi_1). \end{aligned} \quad (2)$$

In order to naturally avoid too-large FCNC interactions of the Higgs bosons to quarks, we impose the Z_2 discrete symmetry [11]: $\Phi_{1(2)} \rightarrow +(-)\Phi_{1(2)}$ (for a recent review see [15]). In such a minimal scenario, the quartic couplings λ_6 and λ_7 vanish, and the CP -odd phase of λ_5 can be rotated away; i.e., there is no explicit CP violation at the tree level.

Assuming that only the neutral components of the two Higgs doublets $\Phi_{1,2}$ develop nonvanishing vacuum expectation values (VEVs), we may parameterize $\Phi_{1,2}$ as follows:

$$\begin{aligned} \Phi_1 &= \begin{pmatrix} \phi_1^+ \\ \frac{1}{\sqrt{2}}(v_1 + \phi_1 + ia_1) \end{pmatrix}, \\ \Phi_2 &= \begin{pmatrix} \phi_2^+ \\ \frac{1}{\sqrt{2}}(v_2 + \phi_2 + ia_2) \end{pmatrix}. \end{aligned} \quad (3)$$

We denote $v_1 \equiv v \cos \beta = v c_\beta$ and $v_2 \equiv v \sin \beta = v s_\beta$, where $v \simeq 246$ GeV is the VEV of the SM Higgs doublet. Extremizing the tree-level scalar potential V^0 leads to the following tadpole conditions:

$$\begin{aligned} T_{\phi_1} &\equiv \left\langle \frac{\partial V^0}{\partial \phi_1} \right\rangle = v_1 \left(\lambda_1 v_1^2 + \frac{1}{2} \lambda_{345} v_2^2 \right) = 0, \\ T_{\phi_2} &\equiv \left\langle \frac{\partial V^0}{\partial \phi_2} \right\rangle = v_2 \left(\lambda_2 v_2^2 + \frac{1}{2} \lambda_{345} v_1^2 \right) = 0, \end{aligned} \quad (4)$$

with $\lambda_{345} \equiv \lambda_3 + \lambda_4 + \lambda_5$. The vanishing of the tadpole parameters $T_{\phi_{1,2}}$ is ensured, provided

$$\frac{\lambda_1}{\lambda_2} = \tan^4 \beta, \quad 2\sqrt{\lambda_1 \lambda_2} = \pm \lambda_{345}. \quad (5)$$

As we will see below, requiring a convex, bounded-from-below potential and a non-negative scalar mass spectrum fixes the \pm sign in front of λ_{345} , which turns out to be minus.

In detail, the tree-level mass spectrum of the charged and neutral Higgs bosons may be calculated as

$$\begin{aligned} V_{\text{mass}}^0 = & (G^+, H^+) \begin{pmatrix} 0 & 0 \\ 0 & M_{H^\pm}^2 \end{pmatrix} \begin{pmatrix} G^- \\ H^- \end{pmatrix} \\ & + \frac{1}{2} (G^0, A) \begin{pmatrix} 0 & 0 \\ 0 & M_A^2 \end{pmatrix} \begin{pmatrix} G^0 \\ A \end{pmatrix} \\ & + \frac{v^2}{2} (\phi_1, \phi_2) \begin{pmatrix} 2\lambda_1 c_\beta^2 & \lambda_{345} c_\beta s_\beta \\ \lambda_{345} c_\beta s_\beta & 2\lambda_2 s_\beta^2 \end{pmatrix} \begin{pmatrix} \phi_1 \\ \phi_2 \end{pmatrix}, \end{aligned} \quad (6)$$

where

$$\begin{pmatrix} \phi_1^- \\ \phi_2^- \end{pmatrix} = \begin{pmatrix} c_\beta & -s_\beta \\ s_\beta & c_\beta \end{pmatrix} \begin{pmatrix} G^- \\ H^- \end{pmatrix}, \quad (7)$$

$$\begin{pmatrix} a_1 \\ a_2 \end{pmatrix} = \begin{pmatrix} c_\beta & -s_\beta \\ s_\beta & c_\beta \end{pmatrix} \begin{pmatrix} G^0 \\ A \end{pmatrix}$$

and

$$M_{H^\pm}^2 = -\frac{1}{2}(\lambda_4 + \lambda_5)v^2, \quad M_A^2 = -\lambda_5 v^2 \quad (8)$$

are the squared masses of the charged and CP -odd Higgs bosons, H^\pm and A , respectively. In addition, we observe that the determinant of the 2×2 CP -even Higgs boson mass matrix vanishes identically, as a consequence of the second tadpole condition in Eq. (5).

The vanishing of the determinant of the CP -even Higgs boson mass matrix signifies the existence of a massless pseudo-Goldstone boson h , arising from the spontaneous breaking of the scaling symmetry along a minimal flat direction of the SI-2HDM potential. In order to determine the flat direction, we perform an orthogonal transformation on the CP -even scalar fields:

$$\begin{pmatrix} \phi_1 \\ \phi_2 \end{pmatrix} = \begin{pmatrix} c_\alpha & -s_\alpha \\ s_\alpha & c_\alpha \end{pmatrix} \begin{pmatrix} H \\ h \end{pmatrix}, \quad (9)$$

so as to render the CP -even scalar mass matrix diagonal, i.e.

$$\begin{pmatrix} c_\alpha & s_\alpha \\ -s_\alpha & c_\alpha \end{pmatrix} \begin{pmatrix} 2\lambda_1 c_\beta^2 & \lambda_{345} c_\beta s_\beta \\ \lambda_{345} c_\beta s_\beta & 2\lambda_2 s_\beta^2 \end{pmatrix} \begin{pmatrix} c_\alpha & -s_\alpha \\ s_\alpha & c_\alpha \end{pmatrix} = \begin{pmatrix} M_H^2/v^2 & 0 \\ 0 & 0 \end{pmatrix}. \quad (10)$$

In this way, we obtain

$$M_H^2 = -\lambda_{345}v^2 = 2\sqrt{\lambda_1\lambda_2}v^2, \quad \sin^2(\alpha - \beta) = 1. \quad (11)$$

Observe that positivity of M_H^2 requires that $\lambda_{345} < 0$. Moreover, the coupling of the massive state (H) to the two vector bosons vanishes, while the coupling of the massless state h is the same as the SM one H_{SM} :

$$\frac{g_{HWW}^2}{g_{H_{\text{SM}}WW}^2} = \cos^2(\alpha - \beta) = 0, \quad (12)$$

$$\frac{g_{hWW}^2}{g_{H_{\text{SM}}WW}^2} = \sin^2(\alpha - \beta) = 1.$$

The flat direction ϕ_{Flat} associated with the massless CP -even scalar h may be expressed in different equivalent forms as follows:

$$\begin{aligned} \phi_{\text{Flat}} &= v + h = v - s_\alpha \phi_1 + c_\alpha \phi_2 \\ &= c_\beta(v_1 + \phi_1) + s_\beta(v_2 + \phi_2), \end{aligned} \quad (13)$$

where we take $\langle \phi_{\text{Flat}} \rangle = v$ and $s_\alpha = -c_\beta$ and $c_\alpha = s_\beta$.

In summary, gathering the results derived above in Eqs. (5), (8), and (11), we have the following constraining set of input parameters:

$$t_\beta^2 = \sqrt{\frac{\lambda_1}{\lambda_2}}, \quad M_H^2 = -(\lambda_3 + \lambda_4 + \lambda_5)v^2 = 2\sqrt{\lambda_1\lambda_2}v^2, \quad (14)$$

$$M_{H^\pm}^2 = -\frac{1}{2}(\lambda_4 + \lambda_5)v^2, \quad M_A^2 = -\lambda_5 v^2.$$

Note that all three tree-level Higgs masses can be determined entirely by the three couplings λ_3 , λ_4 , and λ_5 and the SM VEV v , independently of t_β . We may also invert the relations given in Eq. (14) and determine the five quartic couplings $\lambda_{1,2,3,4,5}$, in terms of v , t_β , and the three Higgs masses:

$$\begin{aligned} \lambda_1 &= \frac{M_H^2}{2v^2} t_\beta^2, & \lambda_2 &= \frac{M_H^2}{2v^2 t_\beta^2}, & \lambda_3 &= \frac{2M_{H^\pm}^2 - M_H^2}{v^2}, \\ \lambda_4 &= \frac{M_A^2 - 2M_{H^\pm}^2}{v^2}, & \lambda_5 &= -\frac{M_A^2}{v^2}. \end{aligned} \quad (15)$$

Finally, it is interesting to comment on the convexity conditions of the Z_2 -invariant 2HDM potential [16,17]. These are given by

$$\begin{aligned} \lambda_1 &> 0, & \lambda_2 &> 0, \\ 2\sqrt{\lambda_1\lambda_2} + \lambda_3 + \min[0, \lambda_4 + \lambda_5, \lambda_4 - \lambda_5] &> 0. \end{aligned} \quad (16)$$

While the first two conditions are easily satisfied, we observe that the third expression of the couplings vanishes identically, since $\min[0, \lambda_4 + \lambda_5, \lambda_4 - \lambda_5] = \lambda_4 + \lambda_5$, and $\lambda_3 + \lambda_4 + \lambda_5 = -2\sqrt{\lambda_1\lambda_2}$ [cf. Eq. (5)]. The vanishing of the third expression signals the existence of a flat direction in the SI-2HDM potential, which gets lifted by radiative corrections as we discuss below.

B. One-loop effective potential

As mentioned above, it is important to consider the quantum effects on the tree-level potential. More explicitly, the one-loop effective potential [1] may be calculated as

$$\begin{aligned} V_{\text{eff}}^{1\text{-loop}} &= \frac{1}{64\pi^2} \left[M_H^4 \left(-\frac{3}{2} + \ln \frac{M_H^2}{Q^2} \right) + M_A^4 \left(-\frac{3}{2} + \ln \frac{M_A^2}{Q^2} \right) \right. \\ &\quad + 2M_{H^\pm}^4 \left(-\frac{3}{2} + \ln \frac{M_{H^\pm}^2}{Q^2} \right) + 6M_W^4 \left(-\frac{5}{6} + \ln \frac{M_W^2}{Q^2} \right) \\ &\quad \left. + 3M_Z^4 \left(-\frac{5}{6} + \ln \frac{M_Z^2}{Q^2} \right) - 12m_t^4 \left(-1 + \ln \frac{m_t^2}{Q^2} \right) \right], \end{aligned} \quad (17)$$

where Q is the RG scale and the background field-dependent masses are given by

$$\begin{aligned}
 M_H^2 &= -2\lambda_{345}(\Phi_1^\dagger\Phi_1 + \Phi_2^\dagger\Phi_2), \\
 M_A^2 &= -2\lambda_5(\Phi_1^\dagger\Phi_1 + \Phi_2^\dagger\Phi_2), \\
 M_{H^\pm}^2 &= -\lambda_{45}(\Phi_1^\dagger\Phi_1 + \Phi_2^\dagger\Phi_2), \\
 M_W^2 &= \frac{g^2}{2}(\Phi_1^\dagger\Phi_1 + \Phi_2^\dagger\Phi_2), \\
 M_Z^2 &= \frac{g^2}{2c_w^2}(\Phi_1^\dagger\Phi_1 + \Phi_2^\dagger\Phi_2), \\
 m_t^2 &= |h_t|^2\Phi_t^\dagger\Phi_t.
 \end{aligned} \tag{18}$$

In the above, we have used the shorthand notation $\lambda_{ij(k)} = \lambda_i + \lambda_j(+\lambda_k)$, with $i, j, k = 3, 4, 5$, and labeled with $I = 1$ or $I = 2$, according to the Z_2 symmetry.

Adding the one-loop effective potential to the tree-level one, i.e. $V = V^0 + V_{\text{eff}}^{1\text{-loop}}$, the tadpole conditions now read

$$\begin{aligned}
 \left\langle \frac{\partial V}{\partial \phi_1} \right\rangle &= T_{\phi_1} + \left\langle \frac{\partial V_{\text{eff}}^{1\text{-loop}}}{\partial \phi_1} \right\rangle = 0, \\
 \left\langle \frac{\partial V}{\partial \phi_2} \right\rangle &= T_{\phi_2} + \left\langle \frac{\partial V_{\text{eff}}^{1\text{-loop}}}{\partial \phi_2} \right\rangle = 0.
 \end{aligned} \tag{19}$$

More explicitly, we obtain

$$\left\langle \frac{\partial V_{\text{eff}}^{1\text{-loop}}}{\partial \phi_i} \right\rangle = \frac{\mathbf{v}_i \mathbf{v}^2}{64\pi^2} \Delta \hat{t}_i, \tag{20}$$

where $\Delta \hat{t}_{1,2}$ are found to be

$$\mathcal{M}_P^2 = \begin{pmatrix} -\lambda_5 \mathbf{v}^2 s_\beta^2 + \frac{T_{\phi_1}}{vc_\beta} + \left\langle \frac{\partial^2 V_{\text{eff}}^{1\text{-loop}}}{\partial a_1^2} \right\rangle & \lambda_5 \mathbf{v}^2 c_\beta s_\beta + \left\langle \frac{\partial^2 V_{\text{eff}}^{1\text{-loop}}}{\partial a_1 \partial a_2} \right\rangle \\ \lambda_5 \mathbf{v}^2 c_\beta s_\beta + \left\langle \frac{\partial^2 V_{\text{eff}}^{1\text{-loop}}}{\partial a_1 \partial a_2} \right\rangle & -\lambda_5 \mathbf{v}^2 c_\beta^2 + \frac{T_{\phi_2}}{vs_\beta} + \left\langle \frac{\partial^2 V_{\text{eff}}^{1\text{-loop}}}{\partial a_2^2} \right\rangle \end{pmatrix}. \tag{24}$$

The VEVs of the double derivatives are found to be

$$\left\langle \frac{\partial^2 V_{\text{eff}}^{1\text{-loop}}}{\partial a_i \partial a_j} \right\rangle = \frac{\mathbf{v}^2}{64\pi^2} \Delta \hat{t}_i \delta_{ij}. \tag{25}$$

Employing the one-loop tadpole conditions [Eq. (22)] along with Eq. (25), we find that the CP -odd mass matrix retains its tree-level form, i.e.

$$\mathcal{M}_P^2 = M_A^2 \begin{pmatrix} s_\beta^2 & -c_\beta s_\beta \\ -c_\beta s_\beta & c_\beta^2 \end{pmatrix} \tag{26}$$

with $M_A = -\lambda_5 \mathbf{v}^2$. In similar fashion, we find that radiative effects do not modify the tree-level structure of the charged Higgs boson mass matrix:

$$\mathcal{M}_S^2 = \begin{pmatrix} 2\lambda_1 \mathbf{v}^2 c_\beta^2 + \frac{T_{\phi_1}}{vc_\beta} + \left\langle \frac{\partial^2 V_{\text{eff}}^{1\text{-loop}}}{\partial \phi_1^2} \right\rangle & \lambda_{345} \mathbf{v}^2 c_\beta s_\beta + \left\langle \frac{\partial^2 V_{\text{eff}}^{1\text{-loop}}}{\partial \phi_1 \partial \phi_2} \right\rangle \\ \lambda_{345} \mathbf{v}^2 c_\beta s_\beta + \left\langle \frac{\partial^2 V_{\text{eff}}^{1\text{-loop}}}{\partial \phi_1 \partial \phi_2} \right\rangle & 2\lambda_2 \mathbf{v}^2 s_\beta^2 + \frac{T_{\phi_2}}{vs_\beta} + \left\langle \frac{\partial^2 V_{\text{eff}}^{1\text{-loop}}}{\partial \phi_2^2} \right\rangle \end{pmatrix}. \tag{29}$$

$$\begin{aligned}
 \Delta \hat{t}_i &= \frac{1}{v^2} \left[4\lambda_{345} M_H^2 \left(1 - \ln \frac{M_H^2}{Q^2} \right) + 4\lambda_5 M_A^2 \left(1 - \ln \frac{M_A^2}{Q^2} \right) \right. \\
 &\quad + 4\lambda_{45} M_{H^\pm}^2 \left(1 - \ln \frac{M_{H^\pm}^2}{Q^2} \right) - 6g^2 M_W^2 \left(\frac{1}{3} - \ln \frac{M_W^2}{Q^2} \right) \\
 &\quad \left. - 3 \frac{g^2}{c_w^2} M_Z^2 \left(\frac{1}{3} - \ln \frac{M_Z^2}{Q^2} \right) + 12|h_t|^2 m_t^2 \left(1 - 2 \ln \frac{m_t^2}{Q^2} \right) \delta_{li} \right].
 \end{aligned} \tag{21}$$

Thus, the one-loop improved tadpole conditions are given by

$$\frac{T_{\phi_1}}{vc_\beta} + \frac{v^2 \Delta \hat{t}_1}{64\pi^2} = 0, \quad \frac{T_{\phi_2}}{vs_\beta} + \frac{v^2 \Delta \hat{t}_2}{64\pi^2} = 0. \tag{22}$$

These conditions can easily be solved for the quartic couplings λ_1 and λ_2 , in terms of the other three couplings $\lambda_{3,4,5}$.

1. Masses of the CP -odd neutral and charged Higgs bosons

The one-loop corrected potential term for the CP -odd scalar mass matrix reads

$$V_{\text{mass}}^{CP\text{-odd}} = \frac{1}{2} (a_1, a_2) \mathcal{M}_P^2 \begin{pmatrix} a_1 \\ a_2 \end{pmatrix}, \tag{23}$$

where

$$V_{\text{mass}}^{H^\pm} = M_{H^\pm}^2 (\phi_1^-, \phi_2^-) \begin{pmatrix} s_\beta^2 & -c_\beta s_\beta \\ -c_\beta s_\beta & c_\beta^2 \end{pmatrix} \begin{pmatrix} \phi_1^+ \\ \phi_2^+ \end{pmatrix}, \tag{27}$$

with $M_{H^\pm}^2 = -\lambda_{45} \mathbf{v}^2 / 2$.

2. Masses and mixing of the CP -even neutral Higgs bosons

One-loop quantum effects give rise to nontrivial contributions to the masses of the CP -even neutral Higgs bosons and their mixing. The one-loop corrected potential term describing these quantum effects is given by

$$V_{\text{mass}}^{CP\text{-even}} = \frac{1}{2} (\phi_1, \phi_2) \mathcal{M}_S^2 \begin{pmatrix} \phi_1 \\ \phi_2 \end{pmatrix}, \tag{28}$$

where \mathcal{M}_S^2 is the 2×2 one-loop improved CP -even mass matrix

Here, the VEVs of the double derivatives of the effective potential with respect to the CP -even scalar fields $\phi_{1,2}$ are calculated to be

$$\left\langle \frac{\partial^2 V_{\text{eff}}^{1\text{-loop}}}{\partial \phi_i \partial \phi_j} \right\rangle = \frac{1}{64\pi^2} (v_i v_j \Delta \hat{m}_{ij}^2 + v^2 \Delta \hat{t}_i \delta_{ij}), \quad (30)$$

with

$$\begin{aligned} \Delta \hat{m}_{ij}^2 \equiv & 8\lambda_{345}^2 \ln \frac{|M_H|^2}{Q^2} + 8\lambda_3^2 \ln \frac{M_A^2}{Q^2} + 4\lambda_{45}^2 \ln \frac{M_{H^\pm}^2}{2} \\ & + g^4 \left(2 + 3 \ln \frac{M_W^2}{Q^2} \right) + \frac{g^4}{2c_W^4} \left(2 + 3 \ln \frac{M_Z^2}{Q^2} \right) \\ & - 12|h_I|^4 \left(1 + 2 \ln \frac{m_t^2}{Q^2} \right) \delta_{ij} \delta_{Ii}. \end{aligned} \quad (31)$$

After implementing the one-loop tadpole conditions [Eq. (22)], the CP -even scalar mass matrix \mathcal{M}_S^2 simplifies to

$$\mathcal{M}_S^2 = v^2 \begin{pmatrix} \left(2\lambda_1 + \frac{\Delta \hat{m}_{11}^2}{64\pi^2} \right) c_\beta^2 & \left(\lambda_{345} + \frac{\Delta \hat{m}_{12}^2}{64\pi^2} \right) c_\beta s_\beta \\ \left(\lambda_{345} + \frac{\Delta \hat{m}_{12}^2}{64\pi^2} \right) c_\beta s_\beta & \left(2\lambda_2 + \frac{\Delta \hat{m}_{22}^2}{64\pi^2} \right) s_\beta^2 \end{pmatrix}. \quad (32)$$

Notice that the top quark contribution in Eq. (31) breaks the universality of $\Delta \hat{m}_{ij}^2$.

In contrast to what happens at the tree level, the diagonalization of the one-loop effective mass matrix \mathcal{M}_S^2 yields two nonvanishing mass eigenvalues. As a consequence of the breaking of the scaling symmetry at the quantum level, the pseudo-Goldstone boson h receives a radiative mass, which could be even larger than the nonzero tree-level mass M_H , for specific choices of parameters. To appropriately describe the radiatively corrected masses and mixing of the CP -even Higgs bosons, we introduce a 2×2 orthogonal matrix O , through

$$(\phi_1, \phi_2)_\alpha^\top = O_{\alpha i} (H_1, H_2)_i^\top, \quad (33)$$

which diagonalizes the CP -even mass matrix as $O^\top \mathcal{M}_S^2 O = \text{diag}(M_{H_1}^2, M_{H_2}^2)$, with the convention $M_{H_1} \leq M_{H_2}$.

In terms of the mixing matrix O , the couplings of the Higgs bosons to the vector bosons are given by

$$\mathcal{L}_{HVV} = gM_W \sum_i g_{H_iVV} \left(H_i W_\mu^+ W^{-\mu} + \frac{1}{2c_W^2} H_i Z_\mu Z^\mu \right), \quad (34)$$

$$\mathcal{L}_{HAZ} = \frac{g}{2c_W} \sum_i g_{H_iAZ} Z^\mu (A \overleftrightarrow{\partial}_\mu H_i), \quad (35)$$

$$\begin{aligned} \mathcal{L}_{HH^\pm W^\mp} = & \frac{g}{2} \left[\sum_i g_{H_i H^\mp W^+} W^{+\mu} (H_i \overleftrightarrow{\partial}_\mu H^-) \right. \\ & \left. + W^{+\mu} (A \overleftrightarrow{\partial}_\mu H^-) + \text{H.c.} \right], \end{aligned} \quad (36)$$

where the action of $\overleftrightarrow{\partial}_\mu$ on two arbitrary functions $f(x)$ and $g(x)$ is defined such that $f(x) \overleftrightarrow{\partial}_\mu g(x) \equiv f(x) \times$

$(\partial_\mu g(x)) - (\partial_\mu f(x))g(x)$. In addition, the reduced couplings that occur in Eqs. (34)–(36) are given by

$$g_{H_iVV} = c_\beta O_{1i} + s_\beta O_{2i}, \quad (37)$$

$$g_{H_iAZ} = g_{H_i H^- W^+} = c_\beta O_{2i} - s_\beta O_{1i},$$

which satisfy the identity

$$g_{H_iAZ}^2 + g_{H_iVV}^2 = 1, \quad (38)$$

for each $i = 1, 2$. The latter implies that $g_{H_1AZ}^2 = g_{H_2VV}^2$ and $g_{H_2AZ}^2 = g_{H_1VV}^2$.

For illustration, we show in Fig. 1 numerical estimates of the CP -even Higgs boson masses M_{H_1, H_2} (left panel) and their couplings $g_{H_iVV}^2$ (right panel), as functions of λ_3 . We have taken $\tan\beta = 1$ and fixed the CP -odd and charged Higgs boson masses to be $M_A = M_{H^\pm} = 400$ GeV. The dependence of the tree-level CP -even Higgs mass $M_H = \sqrt{-\lambda_{345}} v$ on λ_3 is also displayed with a dashed line. We observe that there is a level-crossing phenomenon taking place at the critical value $\lambda_3 = \lambda_3^c \simeq 5.06$, at which $g_{H_1VV}^2 = g_{H_2VV}^2$. For quartic couplings λ_3 smaller than λ_3^c , the lighter state H_1 is mainly SM-like and has the larger coupling to the Z boson, i.e. $g_{H_1VV}^2 > g_{H_2VV}^2$, whereas the heavier boson H_2 has a smaller coupling to Z , and its mass is close to the tree-level value, i.e. $M_{H_2} \sim M_H$. If $\lambda_3 > \lambda_3^c$, the roles of the H_1 and H_2 bosons are exchanged, where the heavier state H_2 becomes the SM-like Higgs boson, with $g_{H_2VV}^2 > g_{H_1VV}^2$, and $M_{H_1} \sim M_H$.

Before closing this section, we comment on our choice of the RG scale:

$$Q = \Lambda_{\text{GW}}, \quad (39)$$

where Λ_{GW} is the so-called Gildener-Weinberg scale [2] which may be determined from the expression

$$\ln \frac{\Lambda_{\text{GW}}}{v} = \frac{\mathcal{A}}{2\mathcal{B}} + \frac{1}{4}. \quad (40)$$

Here, the parameters \mathcal{A} and \mathcal{B} are given by

$$\begin{aligned} \mathcal{A} = & \frac{1}{64\pi^2 v^4} \left[M_H^4 \left(-\frac{3}{2} + \ln \frac{M_H^2}{v^2} \right) + M_A^4 \left(-\frac{3}{2} + \ln \frac{M_A^2}{v^2} \right) \right. \\ & + 2M_{H^\pm}^4 \left(-\frac{3}{2} + \ln \frac{M_{H^\pm}^2}{v^2} \right) + 6M_W^4 \left(-\frac{5}{6} + \ln \frac{M_W^2}{v^2} \right) \\ & \left. + 3M_Z^4 \left(-\frac{5}{6} + \ln \frac{M_Z^2}{v^2} \right) - 12m_t^4 \left(-1 + \ln \frac{m_t^2}{v^2} \right) \right], \\ \mathcal{B} = & \frac{1}{64\pi^2 v^4} (M_H^4 + M_A^4 + 2M_{H^\pm}^4 + 6M_W^4 + 3M_Z^4 - 12m_t^4). \end{aligned} \quad (41)$$

With the choice for the RG scale Q given in Eq. (39), we have checked that the radiative corrections are minimized and the predictions for the masses of the CP -even Higgs bosons exhibit the least sensitivity under small variations of Q around Λ_{GW} . We note that in kinematic regions far from the critical level-crossing point; e.g., for $\lambda_3 \ll \lambda_3^c$, the tree-level relations $M_{H_2} \simeq M_H$, $g_{H_2VV}^2 \simeq 0$, and $g_{H_1VV}^2 \simeq 1$ prove

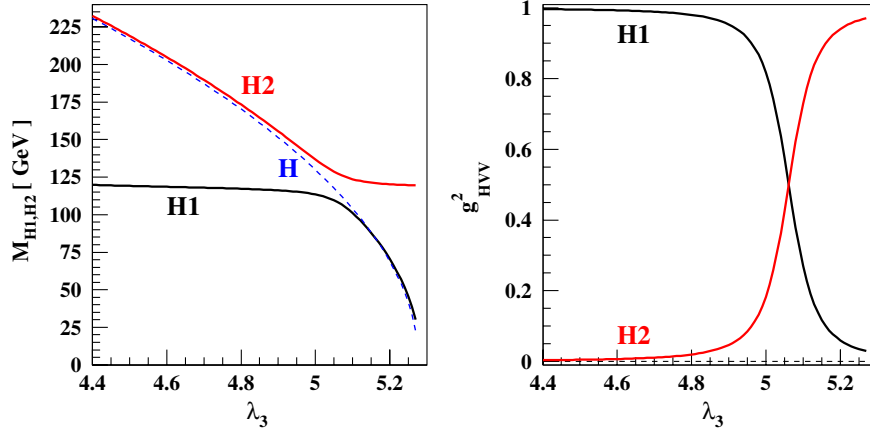


FIG. 1 (color online). The CP -even Higgs masses (left panel) and their couplings $g_{H_i, VV}^2$ (right panel) as functions of λ_3 . We have set $\tan\beta = 1$ and $M_A = M_{H^\pm} = 400$ GeV, corresponding to $\lambda_4 = \lambda_5 \simeq -2.64$. The parameter $M_H = \sqrt{-\lambda_{345}}v$ is the tree-level CP -even Higgs boson mass. The RG scale $Q = \Lambda_{\text{GW}}$ is chosen; see the text for more details.

to be an excellent approximation. Moreover, the radiative mass M_{H_1} of the pseudo-Goldstone boson H_1 may well be approximated by the Gildener-Weinberg mass M_{GW} :

$$M_{H_1}^2 \simeq M_{\text{GW}}^2 \equiv 8\mathcal{B}v^2, \quad (42)$$

where the parameter \mathcal{B} is given by Eq. (41).

III. NUMERICAL ANALYSIS

The SI-2HDM may be parameterized in terms of five independent kinematic parameters. These parameters could be either the five quartic couplings ($\lambda_1, \lambda_2, \lambda_3, \lambda_4, \lambda_5$), or the set $(v, t_\beta, M_H, M_{H^\pm}, M_A)$. At the tree level, the two sets are simply related, by means of Eqs. (14) and (15). For our numerical analysis, we choose to vary the four parameters

$$t_\beta, \quad M_{H^\pm}, \quad M_A, \quad M_H^{\text{eff}}, \quad (43)$$

with $v \simeq 246$ GeV and

$$M_H^{\text{eff}} \equiv M_{H_2} g_{H_1, VV}^2 + M_{H_1} g_{H_2, VV}^2. \quad (44)$$

The latter mass parameter was introduced since its value stays close to that of the tree-level H -boson mass M_H after radiative corrections are included. As discussed in the previous section, the masses of the charged and CP -odd Higgs bosons are not affected by quantum effects, so the couplings λ_4 and λ_5 are determined by the tree-level relations given in Eq. (15). Instead, the couplings $\lambda_{1,2,3}$ receive significant quantum corrections beyond the Born approximation. Explicitly, for given input values of M_H^{eff} and t_β , the couplings $\lambda_{1,2,3}$ can be determined iteratively, after taking into consideration the one-loop tadpole conditions in Eq. (22). For definiteness, we have assumed the type II Yukawa sector for the top quark mass m_t , corresponding to $I = 2$ in Eq. (18). However, our results do not depend on this choice.

A. Theoretical and phenomenological constraints

We now consider several theoretical and phenomenological constraints on the SI-2HDM. These include (i) the

perturbative unitarity bounds [18,19], (ii) the indirect constraints from the electroweak precision data [20], and (iii) the direct constraints from the LEP collider [21] and the LHC [22].

We first consider the constraints obtained by requiring validity of perturbative unitarity [18,19]. For the tree-level unitarity conditions, we closely follow [23]. We observe that the perturbative unitarity constraint is weakest when $\tan\beta = 1$ and becomes stronger as $\tan\beta$ deviates from this value. The reason is that the couplings $\lambda_1 \propto t_\beta^2$ and $\lambda_2 \propto 1/t_\beta^2$ for the present Z_2 -invariant SI-2HDM. Furthermore, at the tree level, the perturbative unitarity bounds are symmetric under the exchange $c_\beta \leftrightarrow s_\beta$, since the eigenvalues of the scattering matrices depend on the combinations of $\lambda_1 + \lambda_2$ and $(\lambda_1 - \lambda_2)^2$, while the other couplings $\lambda_{3,4,5}$ are independent of $\tan\beta$. Specifically, one of the most stringent conditions may come from requiring that the eigenvalue a_+ of the scattering matrices [23] obey the bound

$$a_+ \equiv \frac{1}{16\pi} \left[3(\lambda_1 + \lambda_2) + \sqrt{9(\lambda_1 - \lambda_2)^2 + (2\lambda_3 + \lambda_4)^2} \right] \leq \frac{1}{2}. \quad (45)$$

In view of the above discussion, we only consider regions of parameter space, for which $\tan\beta \geq 1$.

The electroweak oblique corrections to the so-called S , T and U parameters [24,25] provide significant constraints on the quartic couplings of the SI-2HDM. For a vanishing U parameter ($U = 0$), the electroweak oblique parameters are constrained by the following inequality:

$$\frac{(S - \hat{S}_0)^2}{\sigma_S^2} + \frac{(T - \hat{T}_0)^2}{\sigma_T^2} - 2\rho_{ST} \frac{(S - \hat{S}_0)(T - \hat{T}_0)}{\sigma_S \sigma_T} \leq R^2(1 - \rho_{ST}^2), \quad (46)$$

with $R^2 = 2.30, 4.61, 5.99$ and 9.21 , for electroweak precision limits at 68%, 90%, 95% and 99% confidence levels

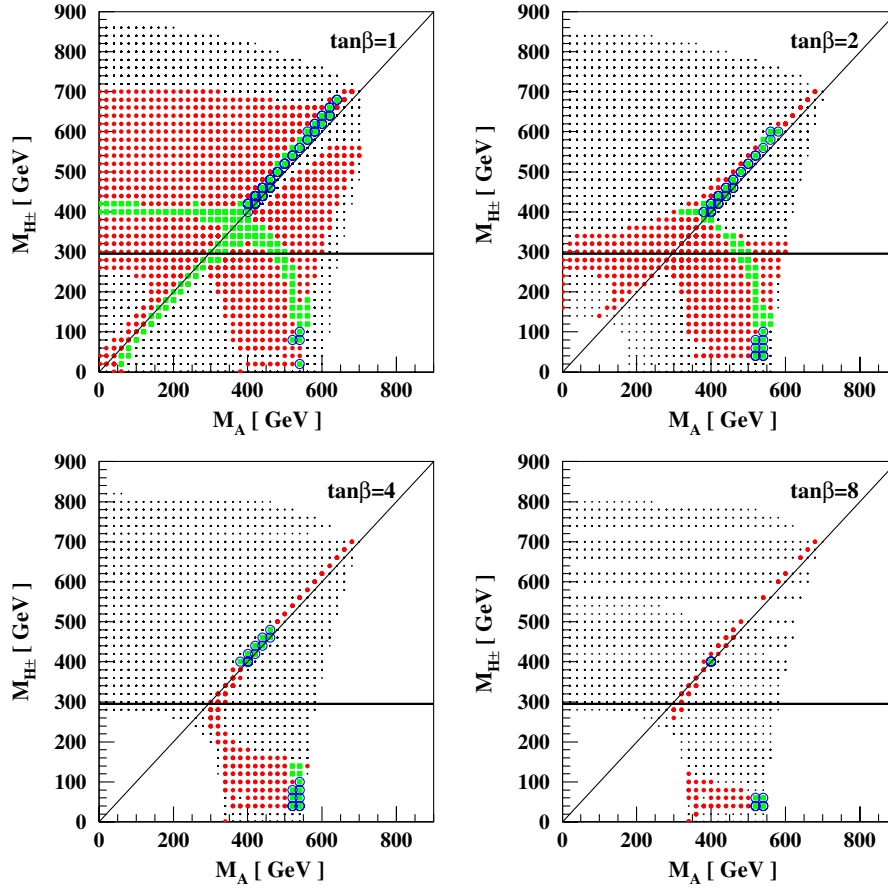


FIG. 2 (color online). The allowed parameter space in the $M_A - M_{H^\pm}$ plane compatible with perturbative unitarity (small black dots) and electroweak precision limits (solid red circles) at the 90% C.L., for $\tan\beta = 1$ (upper left panel), $\tan\beta = 2$ (upper right panel), $\tan\beta = 4$ (lower left panel) and $\tan\beta = 8$ (lower right panel). The region of green squares indicates the allowed area due to the LEP and LHC limits. The open blue circles in the green area single out the region for which $|g_{H_2 VV}| > |g_{H_1 VV}|$. The thick horizontal line gives a lower bound on the charged Higgs mass $M_{H^\pm} \gtrsim 295$ GeV, from the $b \rightarrow s\gamma$ data [31], assuming type II Yukawa couplings.

(C.L.s), respectively. The central values and their standard deviations are given by [20]

$$(\hat{S}_0, \sigma_S) = (0.03, 0.09), \quad (\hat{T}_0, \sigma_T) = (0.07, 0.08), \quad (47)$$

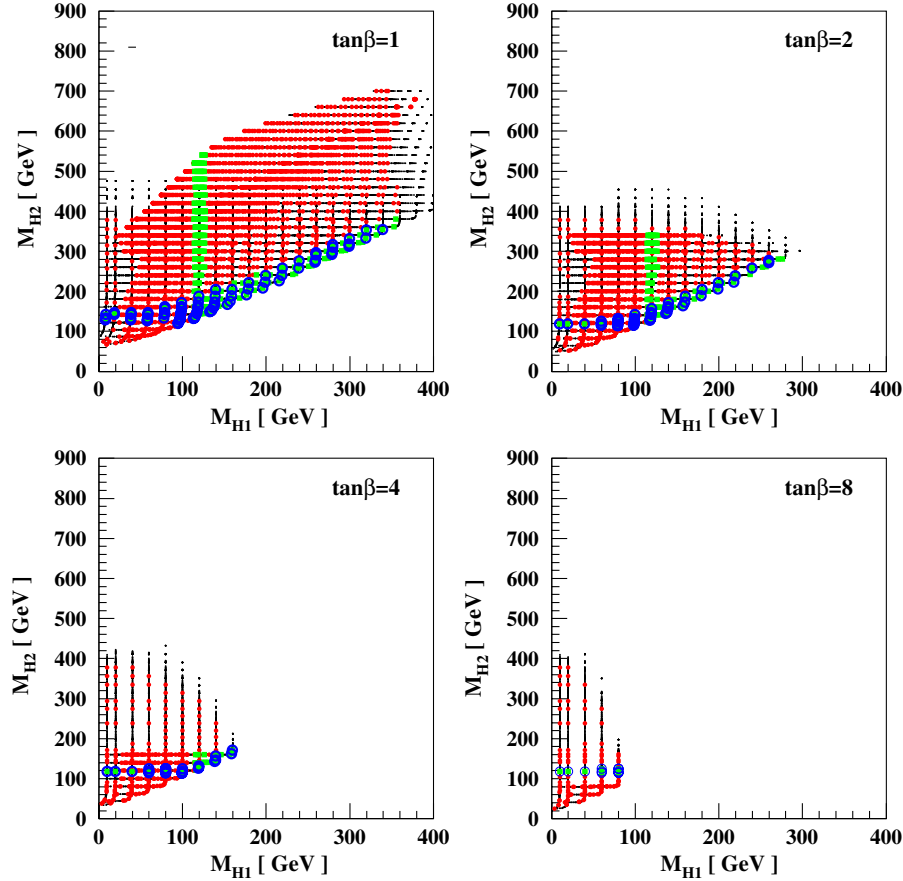
for the value $\rho_{ST} = 0.82$ of the correlation parameter. In our numerical analysis, we apply the 90% C.L. limits.

The SI-2HDM contributions [26] to the S and T parameters may conveniently be expressed as follows:

$$\begin{aligned} S_\Phi &= -\frac{1}{4\pi} \left[(1 + \delta_{\gamma Z}^{H^\pm})^2 F'_\Delta(M_{H^\pm}, M_{H^\pm}) \right. \\ &\quad \left. - \sum_{i=1,2} (g_{H_i AZ} + \delta_Z^{H_i})^2 F'_\Delta(M_{H_i}, M_A) \right], \\ T_\Phi &= -\frac{\sqrt{2}G_F}{16\pi^2 \alpha_{EM}} \left\{ -(1 + \delta_W^A)^2 F_\Delta(M_A, M_{H^\pm}) \right. \\ &\quad + \sum_{i=1,2} \left[(g_{H_i AZ} + \delta_Z^{H_i})^2 F_\Delta(M_{H_i}, M_A) \right. \\ &\quad \left. - (g_{H_i H^- W^+} + \delta_W^{H_i})^2 F_\Delta(M_{H_i}, M_{H^\pm}) \right] \right\}. \quad (48) \end{aligned}$$

In the evaluation of the new-physics parameters S_Φ and T_Φ in Eq. (48), we have dressed the vertex couplings with the dominant one-loop corrections $\mathcal{O}(\lambda^2/16\pi^2)$, where λ symbolizes a generic quartic coupling $\lambda_{1,2,3,4,5}$. These additional λ^2 -dependent contributions are denoted as $\delta_{\gamma Z}^{H^\pm}$, $\delta_Z^{H_i, H_2}$ and δ_W^{A, H_1, H_2} , and become rather significant for quartic couplings $|\lambda| > 1$. Their explicit analytic forms are presented in the Appendix A.

On the other hand, the analytic form of the one-loop functions $F_\Delta(m_1, m_2)$ and $F'_\Delta(m_1, m_2)$ may be found in [27]. Here we simply quote some of their key properties: $F_\Delta(m_1, m_2) = F_\Delta(m_2, m_1)$, $F'_\Delta(m_1, m_2) = F'_\Delta(m_2, m_1)$ and $F_\Delta(m, m) = 0$. If the λ^2 -dependent vertex corrections are ignored, then S_Φ and T_Φ become independent of $\tan\beta$ and symmetric under the exchange $M_A \leftrightarrow M_{H_2}$, since $g_{H_2 AZ}^2 = g_{H_2 H^- W^+}^2 = g_{H_1 VV}^2 = 1$ and $g_{H_1 AZ}^2 = g_{H_1 H^- W^+}^2 = g_{H_2 VV}^2 = 0$ at the tree level in the SI-2HDM. Finally, it is interesting to observe that T_Φ vanishes identically in the limit $M_A \rightarrow M_{H^\pm}$, or equivalently when $\lambda_4 \rightarrow \lambda_5$. In this limit, the SI-2HDM realizes an unbroken $SO(3)$ custodial symmetry in the bilinear scalar field space of $SO(5)$, according to a


 FIG. 3 (color online). The same as in Fig. 2, but in the $M_{H_1} - M_{H_2}$ plane.

recent classification of the 2HDM potential [28,29]. Since this symmetry remains unbroken even by the inclusion of λ -dependent vertex corrections, the electroweak parameter T_Φ still vanishes.

The total contribution to the electroweak S and T parameters is given by the sums $S = S_{\text{SM}} + S_\Phi$ and $T = T_{\text{SM}} + T_\Phi$. For the SM contribution, we have employed the parameterizations [30]

$$\begin{aligned} S_{\text{SM}} &= -0.007x_t + 0.091x_h - 0.010x_h^2, \\ T_{\text{SM}} &= (0.130 - 0.003x_h)x_t + 0.003x_t^2 - 0.079x_h \\ &\quad - 0.028x_h^2 + 0.0026x_h^3, \end{aligned} \quad (49)$$

with $x_t = (m_t/\text{GeV} - 173)/10$ and $x_h = \ln(M_{H_{\text{SM}}}/117 \text{ GeV})$, where $M_{H_{\text{SM}}} \equiv M_{H_1}g_{H_1VV}^2 + M_{H_2}g_{H_2VV}^2$. This last expression approximates the mass of the SM Higgs boson fairly well over the whole region of the parameter space.

The recent LHC data pertinent to SM Higgs boson searches provide important constraints on the kinematic parameters of the SI-2HDM. In our numerical analysis, we derive conservative limits by taking that either $g_{H_1VV}^2 = 1$ or $g_{H_2VV}^2 = 1$. To this end, we consider the 95% C.L. exclusion limits on the SM Higgs boson mass $M_{H_{\text{SM}}}$, as quoted by the CMS and ATLAS collaborations [22]:

CMS: 127 GeV–600 GeV,

ATLAS: 112.7 GeV–115.5 GeV, 131 GeV–453 GeV.

(50)

Combining the above CMS and ATLAS results, the following LHC exclusion limits on the Higgs masses may be deduced:

$$\begin{aligned} 127 < M_{H_1}/\text{GeV} < 600, & \quad \text{when } g_{H_1VV}^2 \geq 0.99, \\ 127 < M_{H_2}/\text{GeV} < 600, & \quad \text{when } g_{H_2VV}^2 \geq 0.99. \end{aligned}$$

More precise limits may be derived by calculating the production cross sections for each Higgs search channel, in conjunction with the limits on the ratio $\sigma/\sigma_{\text{SM}}$. We leave this issue to our experimental colleagues for more detailed analyses. Finally, we have included the LEP limits according to [21].

B. Numerical predictions

We start our numerical analysis by showing in Fig. 2 the allowed parameter space in the $M_A - M_{H^\pm}$ plane, which is compatible with perturbative unitarity (small black dots) and electroweak precision limits (solid red circles) at the 90% C.L., for four values of $\tan\beta$: $\tan\beta = 1$ (upper left panel), $\tan\beta = 2$ (upper right panel), $\tan\beta = 4$ (lower left

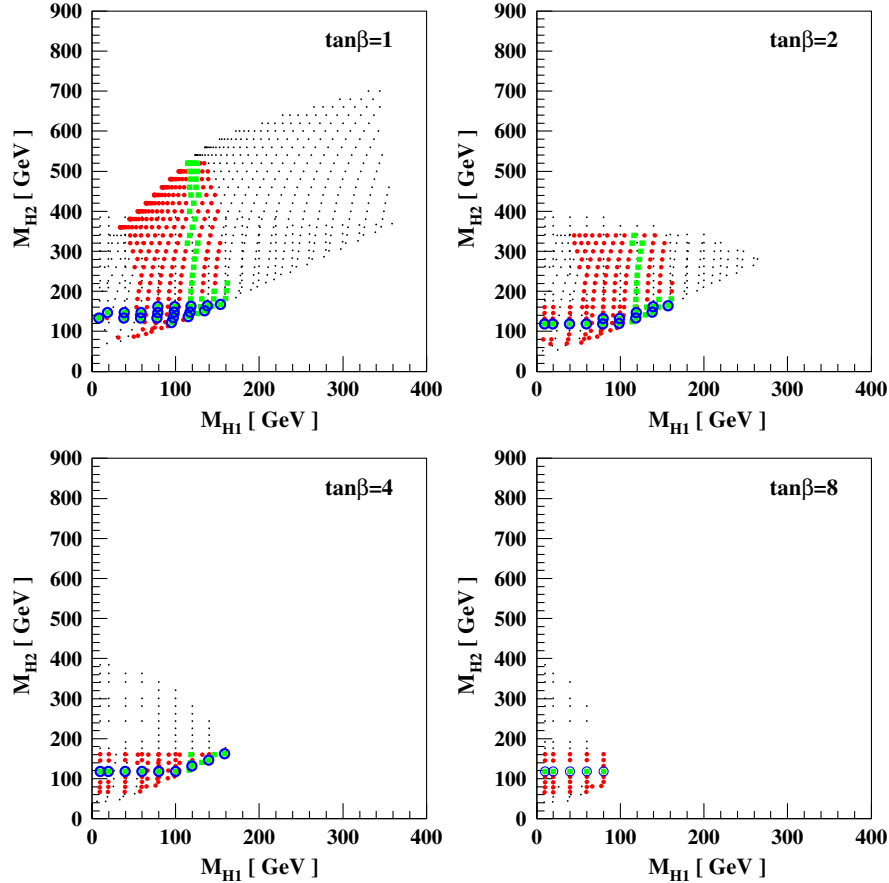


FIG. 4 (color online). The same as in Fig. 3, but with the restriction $M_{H^\pm} = M_A$.

panel) and $\tan\beta = 8$ (lower right panel). Moreover, the region of green squares in Fig. 2 indicates the allowed area due to the LEP and LHC mass limits on a SM-like Higgs boson. The open blue circles in the green area highlight the region governed by the coupling hierarchy $|g_{H_2VV}| > |g_{H_1VV}|$. The thick horizontal line that appears in each panel of Fig. 2 displays the lower bound on the charged Higgs boson mass, $M_{H^\pm} \gtrsim 295$ GeV, which is derived from the $b \rightarrow s\gamma$ data [31], assuming a type II Yukawa coupling model.

From Fig. 2, we observe that the combined constraints get weaker for low values of $\tan\beta$, with $\tan\beta = 1$ giving the weakest exclusion limits. The allowed parameter space is dominated by the points for which $M_{H^\pm} \approx M_A$ and $M_{H^\pm} \approx M_{H_2}$ and centered around 400 GeV. This may be understood as follows. The direct constraints from LEP and the LHC data restrict the mass of the SM-like Higgs boson to lie in the region between 114.4 GeV and 127 GeV. This is close to the value 117 GeV, for which S_{SM} and T_{SM} almost vanish. On the other hand, the contributions from the heavier Higgs bosons to the T parameter are significant, unless their masses stay close to the custodial symmetric limit, where $M_{H^\pm} \approx M_A$. Alternatively, an accidental suppression of the T_Φ parameter takes place when $M_{H^\pm} \approx M_{H_2}$. If in view of the electroweak precision constraints we take $M_{H^\pm} = M_A = M_{H_2} \equiv M_X$, then the relation $M_{H_1}^2 \approx M_{\text{GW}}^2 = 8\mathcal{B}v^2$ [cf. Eq. (43)] leads typically to

$$M_X^4 \sim \frac{1}{4}(8\pi^2 v^2 M_{H_1}^2 - 6M_W^4 - 3M_Z^4 + 12m_t^4). \quad (51)$$

Thus, for $M_{H_1} \sim 120$ GeV, one obtains an approximate estimate of $M_X \sim 400$ GeV.

Let us now look more closely at how each constraint acts on the parameter space. The requirement of perturbative unitarity (p.u.) constrains the masses of the charged and CP -odd Higgs bosons as follows:

$$M_{H^\pm}^{\text{p.u.}} \lesssim 850 \text{ GeV}, \quad M_A^{\text{p.u.}} \lesssim 700 \text{ GeV}. \quad (52)$$

Note that these upper bounds are almost independent of $\tan\beta$. Instead, the perturbative unitarity limit on M_H depends crucially on $\tan\beta$, which becomes stronger for large values of $\tan\beta$. This is a direct consequence of the relation $\lambda_1 \approx M_H^2 t_\beta^2 / 2v^2$ and the perturbative bound imposed on λ_1 . Therefore, the regions with small M_{H^\pm} and/or M_A are excluded, since $M_{H_1}^2$ becomes negative. The reason is that for $|g_{H_1VV}| > |g_{H_2VV}|$, one has the relation $M_{H_1}^2 \approx M_{\text{GW}}^2 = 8\mathcal{B}v^2$, and the one-loop parameter \mathcal{B} given in Eq. (41) should be positive.

The electroweak (e.w.) oblique parameters offer additional constraints on the scalar masses and on $\tan\beta$. Specifically, the mass limits become stronger for larger values of $\tan\beta$, i.e.

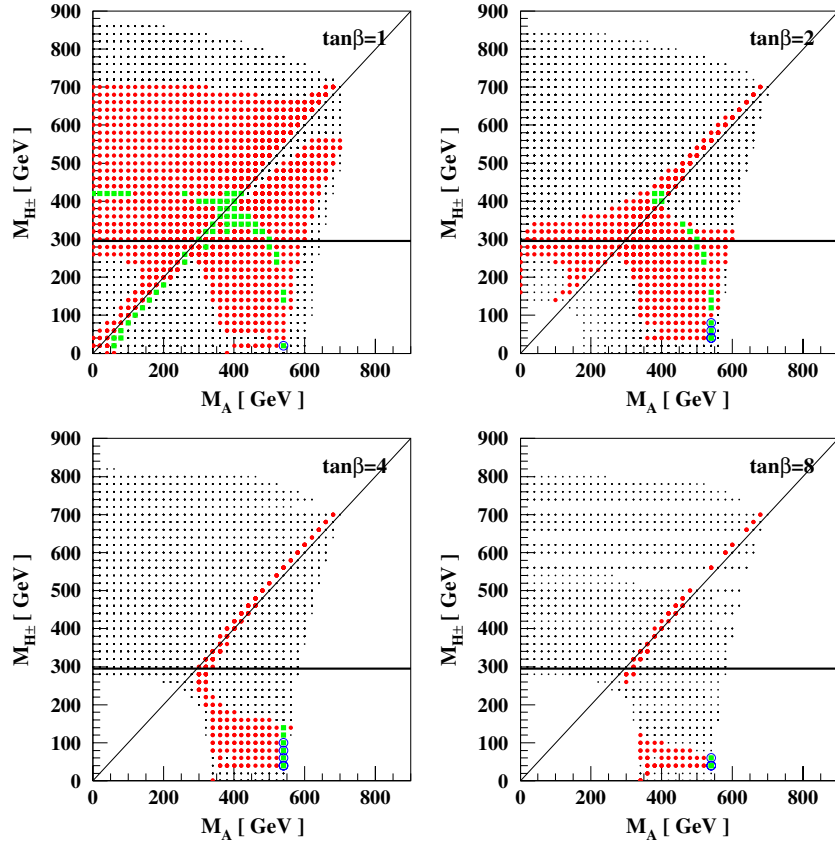


FIG. 5 (color online). The same as in Fig. 2, but restricting either M_{H_1} or M_{H_2} to lie between 123 and 127 GeV.

$$\begin{aligned}
 \tan\beta = 1: & M_{H^\pm}^{\text{p.u.}\oplus\text{e.w.}} \lesssim 700 \text{ GeV}, & M_A^{\text{p.u.}\oplus\text{e.w.}} & \lesssim 700 \text{ GeV}, \\
 \tan\beta = 2: & M_{H^\pm}^{\text{p.u.}\oplus\text{e.w.}} \lesssim 700 \text{ GeV}, & M_A^{\text{p.u.}\oplus\text{e.w.}} & \lesssim 700 \text{ GeV}, \\
 \tan\beta = 4: & M_{H^\pm}^{\text{p.u.}\oplus\text{e.w.}} \lesssim 700 \text{ GeV}, & 300 \text{ GeV} \lesssim M_A^{\text{p.u.}\oplus\text{e.w.}} & \lesssim 700 \text{ GeV}, \\
 \tan\beta = 8: & M_{H^\pm}^{\text{p.u.}\oplus\text{e.w.}} \lesssim 700 \text{ GeV}, & 300 \text{ GeV} \lesssim M_A^{\text{p.u.}\oplus\text{e.w.}} & \lesssim 700 \text{ GeV},
 \end{aligned} \tag{53}$$

where the superscript p.u. \oplus e.w indicates the simultaneous implementation of limits due to perturbative unitarity and the electroweak precision S and T parameters.

As a final constraint, we consider the direct LEP and LHC limits on a SM-like Higgs boson mass. If we combine these limits with the bound derived on the charged Higgs mass $M_{H^\pm} \gtrsim 295$ GeV from the $b \rightarrow s\gamma$ data [31], we find that

$$\begin{aligned}
 \tan\beta = 1: & 295 \text{ GeV} \lesssim M_{H^\pm} \lesssim 680 \text{ GeV}, & M_A & \lesssim 650 \text{ GeV}, \\
 \tan\beta = 2: & 295 \text{ GeV} \lesssim M_{H^\pm} \lesssim 600 \text{ GeV}, & 320 \text{ GeV} \lesssim M_A & \lesssim 580 \text{ GeV}, \\
 \tan\beta = 4: & M_{H^\pm} \simeq M_A \sim 380\text{--}480 \text{ GeV}, \\
 \tan\beta = 8: & M_{H^\pm} \simeq M_A \sim 400 \text{ GeV}.
 \end{aligned} \tag{54}$$

Finally, it is worth remarking that only the scenarios with $|g_{H_2 VV}| > |g_{H_1 VV}|$, which are highlighted by blue circles in the plots, are allowed for larger values of $\tan\beta$; e.g., up to $\tan\beta = 8$.

In Fig. 3, we present the allowed parameter space in the $M_{H_1} - M_{H_2}$ plane. The allowed parameter space decreases when $\tan\beta$ deviates from 1. When $\tan\beta = 1$, we find there exist three favorable mass regions:

$$\begin{aligned}
 \text{I. } M_{H_1} > 127 \text{ GeV: } & M_{H_1}^{t_{\beta=1}} \sim 127\text{--}350 \text{ GeV}, & M_{H_2}^{t_{\beta=1}} & \sim 140\text{--}380 \text{ GeV}, \\
 \text{II. } M_{H_1} = 114\text{--}127 \text{ GeV: } & M_{H_1}^{t_{\beta=1}} = 114\text{--}127 \text{ GeV}, & M_{H_2}^{t_{\beta=1}} & \sim 140\text{--}550 \text{ GeV}, \\
 \text{III. } M_{H_1} < 114 \text{ GeV: } & M_{H_1}^{t_{\beta=1}} < 114 \text{ GeV}, & M_{H_2}^{t_{\beta=1}} & \sim 120\text{--}170 \text{ GeV}.
 \end{aligned} \tag{55}$$

In region I, the mixing between the H_1 and H_2 scalars is significant with $M_{H_1} \sim M_{H_2}$. In this case, the LHC exclusion limits on a SM-like Higgs boson may not be straightforwardly applicable. For this reason, our obtained limits should be regarded as conservative in this case. On the other hand, there is no lower limit on the H_1 boson lying in region III with $g_{H_1, VV}^2 \ll 1$, thus allowing for a very light scalar to have escaped detection at the LEP II collider. For the larger values of $\tan\beta$, scenarios with $g_{H_1, VV}^2 \ll g_{H_2, VV}^2$ are becoming more likely. For instance, when $\tan\beta = 8$, we find

$$M_{H_1}^{t_\beta=8} \lesssim 80 \text{ GeV}, \quad M_{H_2}^{t_\beta=8} \sim 118 \text{ GeV}. \quad (57)$$

Figure 4 shows the allowed parameter space in the $M_{H_1} - M_{H_2}$ plane for the custodial symmetric scenario with $M_{H^\pm} = M_A$. As explained in the previous subsection, T_Φ vanishes identically in this scenario, because $F_\Delta(M_A, M_{H^\pm}) = 0$ and $\delta_Z^{H_i} = \delta_W^{H_i}$. Therefore, the masses M_{H_1} or M_{H_2} must be close to 120 GeV, in order for the SM contribution T_{SM} to remain acceptably small.

Motivated by the 2.3σ excess of a positive SM Higgs signal corresponding to $M_{H_{\text{SM}}} \sim 125$ GeV [22], we show in Fig. 5 the allowed regions in the $M_A - M_{H^\pm}$ plane, where either the H_1 boson or the H_2 boson mass is restricted to lie in the interval (123,127) GeV. Taking into account the lower bound on the charged Higgs boson mass, $M_{H^\pm} \sim 295$ GeV, derived from $b \rightarrow s\gamma$ data, we find that all viable scenarios must have $|g_{H_1, VV}| > |g_{H_2, VV}|$ and $\tan\beta \leq 2$. In this case, we find the following three possible scenarios:

- (i) $M_{H_2} \sim M_A \sim 400$ GeV with $M_{H^\pm} \lesssim 420$ GeV
- (ii) $M_A \lesssim 100$ GeV with $M_{H^\pm} \sim M_{H_2} \sim 400$ GeV
- (iii) $M_{H_2} \lesssim 180$ GeV with $M_{H^\pm} \sim M_A \sim 400$ GeV

In conclusion, if $M_{H_1} \sim 125$ GeV, viable scenarios of the SI-2HDM generically have at least two heavy Higgs bosons of $\sim 400 - \text{GeV}$ mass and favor low values of $t_\beta \sim 1$.

IV. CONCLUSIONS

We have studied the Higgs sector of a classical scale invariant realization of the two Higgs doublet model (SI-2HDM). Such a model may provide a minimal and calculable solution to the well-known gauge hierarchy problem. To naturally suppress flavor off-diagonal interactions of the Higgs bosons to quarks, we have imposed the usual Z_2 symmetry on the SI-2HDM potential. In this case, the SI-2HDM scalar potential only depends on the five quartic couplings λ_{1-5} , and hence it becomes very predictive.

The classical scale symmetry of the SI-2HDM is explicitly broken by quantum loop effects due to gauge interactions, Higgs self-couplings and top quark Yukawa couplings. To take account of these effects, we have calculated the one-loop effective potential and evaluated the radiatively corrected masses of the CP -even Higgs bosons

and their mixing. Unlike the CP -even Higgs sector, we have found that the CP -odd and charged Higgs mass matrices retain their tree-level form. In addition to the CP -even Higgs masses, radiative effects may drastically modify the Higgs couplings to the Z boson, through an effective $H_1 - H_2$ mixing. Our analysis has revealed that a critical value of the coupling λ_3^c exists, for which $|g_{H_1, VV}| = |g_{H_2, VV}|$. Depending on the value of λ_3 , a level-crossing phenomenon occurs for both the H_1 and H_2 masses and their couplings to the Z boson. For $\lambda_3 < \lambda_3^c$, the lighter state H_1 behaves like the SM Higgs boson, with $g_{H_1, VV}^2 \sim 1$, and its mass is well approximated by the Gildener-Weinberg mass $M_{H_1} \sim M_{\text{GW}}$, while $M_{H_2} \sim M_H$. Instead, if $\lambda_3 > \lambda_3^c$, the heavier state H_2 becomes SM-like with $g_{H_2, VV}^2 \sim 1$, and its mass is approximately given by $M_{H_2} \sim M_{\text{GW}}$, while $M_{H_1} \sim M_H$.

In our numerical analysis, we have imposed three basic theoretical and phenomenological constraints on the SI-2HDM: (i) the requirement of validity of perturbative unitarity, (ii) the indirect constraints from the electroweak precision data and (iii) the direct Higgs search constraints from the LEP collider and the LHC. At large $\tan\beta$, the perturbative unitarity bounds and the indirect constraints become rather strong. In conjunction with the existing LEP and the current LHC limits on the SM Higgs boson mass, the electroweak T -parameter constraints reduce the theoretically allowed parameter space into two smaller regions, governed by the approximate restrictions: $M_{H^\pm} \sim M_A$ or $M_{H^\pm} \sim M_{H_2}$. In this context, our analysis has shown that the Higgs boson masses obey the following upper limits:

$$\begin{aligned} M_{H_1} &\lesssim 350 \text{ GeV}, & M_{H_2} &\lesssim 550 \text{ GeV}, \\ M_A &\lesssim 650 \text{ GeV}, & M_{H^\pm} &\lesssim 680 \text{ GeV}. \end{aligned}$$

The above bounds hold for low values of $\tan\beta \sim 1$. For $\tan\beta \geq 4$, the masses may be further restricted, with $M_{H^\pm} \approx M_A \sim 400 - 500$ GeV. In addition, the heavier CP -even state H_2 becomes more SM-like with $M_{H_2} \sim 114 - 170$ GeV and $M_{H_1} \lesssim 160$ GeV.

Motivated by the 2.3σ excess for a Higgs mass around 125 GeV at the LHC, we have extended our analysis by including the bound on the charged Higgs mass $M_{H^\pm} \leq 295$ GeV from the $b \rightarrow s\gamma$ data. In this case, we have found that $\tan\beta \sim 1$ and the lightest Higgs boson is SM-like, with $M_{H_1} = M_{H_{\text{SM}}} \approx 125$ GeV. The heavier CP -even Higgs boson H_2 can be lighter than 180 GeV when $M_{H^\pm} \sim M_A \sim 400$ GeV. On the other hand, the CP -odd scalar A can be lighter than 100 GeV when $M_{H^\pm} \sim M_{H_2} \sim 400$ GeV. Otherwise, the pronounced mass region for H_2 and A is mainly around 400 GeV with $M_{H^\pm} \lesssim 420$ GeV. We may therefore conclude that, if $M_{H_{\text{SM}}} \sim 125$ GeV, there are at least two heavy Higgs bosons with masses close to 400 GeV and the third one below ~ 500 GeV in the SI-2HDM.

At the LHC, the heavy neutral Higgs bosons H_2 and A , with masses $M_{H_{2,A}} \sim 400$ GeV, are expected to be mainly

produced via gluon-gluon fusion, where the Higgs pair production channel might be also relevant. In general, the search strategies for the Higgs bosons H_2 , A and H^\pm will depend on the type of the Yukawa sector assumed. Moreover, the detection of possible light Higgs bosons with masses below 100 GeV and suppressed couplings to vector bosons becomes a difficult issue. A detailed investigation of the possible search strategies may be given elsewhere.

Another problem that needs to be addressed in detail within the SI-2HDM pertains to the natural implementation of light neutrino masses. If the theory is extended with right-handed neutrinos, then light neutrino masses can only be incorporated in the theory in a SI manner, via the standard but very small Dirac Yukawa couplings. However, in the presence of extra singlets or triplets, further possibilities arise to naturally explain the smallness of the light neutrino masses, along the lines presented in [9,32,33]. It would be interesting to investigate the phenomenological implications of such extensions of the SI-2HDM in a future communication.

ACKNOWLEDGMENTS

The work of J. S. L. is supported in part by the NSC of Taiwan under Grant. No. 100-2112-M-007-023-MY3) and the work of A. P. by the Lancaster-Manchester-Sheffield Consortium for Fundamental Physics under STFC Grant No. ST/J000418/1.

APPENDIX: VERTEX CORRECTIONS AND TRILINEAR HIGGS COUPLINGS

In this appendix we calculate the one-loop quantum corrections $\mathcal{O}(\lambda_{1-5}^2)$ to the gauge-invariant, transverse part of the gauge couplings to neutral and charged Higgs bosons. These quantum effects get enhanced for large

potential couplings and should be included next to the tree-level contributions. Our calculation is performed in the effective potential limit, in which all external momenta squared are assumed to vanish.

The radiative corrections to the $Z - H^\pm - H^\mp$ and $\gamma - H^\pm - H^\mp$ couplings are the same. In detail, these are given by

$$\begin{aligned} \delta_Z^{H^\pm} &= \delta_\gamma^{H^\pm} \equiv \delta_{\gamma Z}^{H^\pm} \\ &= \frac{v^2}{16\pi^2} \sum_{j=1,2} \lambda_{H_j H^- H^+}^2 f_V(M_{H^\pm}^2, M_{H_j}^2, M_{H^\pm}^2). \end{aligned} \quad (\text{A1})$$

Here, $f_V(m_1^2, m_2^2, m_3^2)$ is the one-loop vertex function, which has been calculated to be

$$\begin{aligned} f_V(m_1^2, m_2^2, m_3^2) &= \frac{1}{(m_3^2 - m_1^2)} \left[\frac{m_3^2}{2(m_2^2 - m_3^2)} - \frac{m_1^2}{2(m_2^2 - m_1^2)} \right. \\ &\quad + \frac{m_3^4}{2(m_2^2 - m_3^2)^2} \ln\left(\frac{m_3^2}{m_2^2}\right) \\ &\quad \left. - \frac{m_1^4}{2(m_2^2 - m_1^2)^2} \ln\left(\frac{m_1^2}{m_2^2}\right) \right], \end{aligned}$$

with $f_V(m^2, m^2, m^2) = 1/(6m^2)$. Likewise, the one-loop corrections to the $H_i - A - Z$ couplings are given by

$$\begin{aligned} \delta_Z^{H_i} &= \frac{v^2}{16\pi^2} \left[-\lambda_{H_i AA} \sum_{j=1,2} g_{H_j AZ} \lambda_{H_j AA} f_V(M_A^2, M_A^2, M_{H_j}^2) \right. \\ &\quad + \sum_{(j,k)=(1,1)}^{(1,2),(2,1),(2,2)} \lambda_{H_i H_j H_k} g_{H_j AZ} \lambda_{H_k AA} f_V(M_{H_j}^2, M_{H_k}^2, M_A^2) \left. \right]. \end{aligned} \quad (\text{A2})$$

By analogy, the one-loop corrections to the $A - H^\pm - W^\mp$ and $H_i - H^\pm - W^\mp$ couplings are given by

$$\begin{aligned} \delta_W^A &= \frac{v^2}{16\pi^2} \left[\sum_{j=1,2} \lambda_{H_j AA} \lambda_{H_j H^- H^+} f_V(M_A^2, M_{H_j}^2, M_{H^\pm}^2) \right], \\ \delta_W^{H_i} &= \frac{v^2}{16\pi^2} \left[-\lambda_{H_i H^- H^+} \sum_{j=1,2} g_{H_j H^- W^+} \lambda_{H_j H^- H^+} f_V(M_{H^\pm}^2, M_{H^\pm}^2, M_{H_j}^2) \right. \\ &\quad \left. + \sum_{(j,k)=(1,1)}^{(1,2),(2,1),(2,2)} \lambda_{H_i H_j H_k} g_{H_j H^- W^+} \lambda_{H_k H^- H^+} f_V(M_{H_j}^2, M_{H_k}^2, M_{H^\pm}^2) \right]. \end{aligned} \quad (\text{A3})$$

Notice that $\delta_Z^{H_i} = \delta_W^{H_i}$ in the custodial symmetric limit: $M_A = M_{H^\pm}$ or $\lambda_4 = \lambda_5$, since $\lambda_{H_i AA} = \lambda_{H_i H^\pm H^\mp}$.

The Higgs potential terms describing the trilinear Higgs interactions may be written down as follows:

$$\begin{aligned} V_{\text{Trilinear}} &= v \left(\frac{\lambda_{H_1 H_1 H_1}}{6} H_1^3 + \frac{\lambda_{H_1 H_1 H_2}}{2} H_1^2 H_2 + \frac{\lambda_{H_1 H_2 H_2}}{2} H_1 H_2^2 + \frac{\lambda_{H_2 H_2 H_2}}{6} H_2^3 + \frac{\lambda_{H_1 AA}}{2} H_1 AA + \frac{\lambda_{H_2 AA}}{2} H_2 AA \right. \\ &\quad \left. + \lambda_{H_1 G^0 A} H_1 G^0 A + \lambda_{H_2 G^0 A} H_2 G^0 A + \frac{\lambda_{H_1 G^0 G^0}}{2} H_1 G^0 G^0 + \frac{\lambda_{H_2 G^0 G^0}}{2} H_2 G^0 G^0 \right) \\ &\quad + v \sum_{i=1,2} [\lambda_{H_i G^- G^+} H_i G^- G^+ + \lambda_{H_i G^\mp H^\pm} H_i (G^- H^+ + G^+ H^-) + \lambda_{H_i H^- H^+} H_i H^- H^+], \end{aligned} \quad (\text{A4})$$

where the trilinear self-couplings of the CP -even Higgs bosons are

$$\begin{aligned}\lambda_{H_1 H_1 H_1} &= 6(O_{11}^3 \lambda_{\phi_1 \phi_1 \phi_1} + O_{11}^2 O_{21} \lambda_{\phi_1 \phi_1 \phi_2} + O_{11} O_{21}^2 \lambda_{\phi_1 \phi_2 \phi_2} + O_{21}^3 \lambda_{\phi_2 \phi_2 \phi_2}), \\ \lambda_{H_1 H_1 H_2} &= 6O_{11}^2 O_{12} \lambda_{\phi_1 \phi_1 \phi_1} + 2(O_{11}^2 O_{22} + 2O_{11} O_{12} O_{21}) \lambda_{\phi_1 \phi_1 \phi_2} + 2(O_{12} O_{21}^2 + 2O_{11} O_{21} O_{22}) \lambda_{\phi_1 \phi_2 \phi_2} + 6O_{21}^2 O_{22} \lambda_{\phi_2 \phi_2 \phi_2}, \\ \lambda_{H_1 H_2 H_2} &= 6O_{11} O_{12}^2 \lambda_{\phi_1 \phi_1 \phi_1} + 2(O_{12}^2 O_{21} + 2O_{11} O_{12} O_{22}) \lambda_{\phi_1 \phi_1 \phi_2} + 2(O_{11} O_{22}^2 + 2O_{12} O_{21} O_{22}) \lambda_{\phi_1 \phi_2 \phi_2} + 6O_{21} O_{22}^2 \lambda_{\phi_2 \phi_2 \phi_2}, \\ \lambda_{H_2 H_2 H_2} &= 6(O_{12}^3 \lambda_{\phi_1 \phi_1 \phi_1} + O_{12}^2 O_{22} \lambda_{\phi_1 \phi_1 \phi_2} + O_{12} O_{22}^2 \lambda_{\phi_1 \phi_2 \phi_2} + O_{22}^3 \lambda_{\phi_2 \phi_2 \phi_2}).\end{aligned}\quad (\text{A5})$$

In addition, the trilinear couplings involving one CP -even Higgs boson and two CP -odd scalars may be cast into the form:

$$\lambda_{H,XY} = N_{XY}(O_{1i} \lambda_{\phi_1 XY} + O_{2i} \lambda_{\phi_2 XY}), \quad (\text{A6})$$

with $(XY, N_{XY}) = (AA, 2), (G^0 A, 1), (G^0 G^0, 2)$.

Finally, the trilinear CP -even Higgs couplings with the charged Higgs bosons H^\pm may be expressed as follows:

$$\lambda_{H_i X' Y'} = O_{1i} \lambda_{\phi_1 X' Y'} + O_{2i} \lambda_{\phi_2 X' Y'}, \quad (\text{A7})$$

with $X' Y' = G^- G^+, G^\mp H^\pm$ and $H^- H^+$. The trilinear couplings in the basis of weak eigenstates are given by

$$\begin{aligned}\lambda_{\phi_1 \phi_1 \phi_1} &= \lambda_1 c_\beta, & \lambda_{\phi_1 \phi_1 \phi_2} &= \frac{\lambda_{345}}{2} s_\beta, & \lambda_{\phi_1 \phi_2 \phi_2} &= \frac{\lambda_{345}}{2} c_\beta, & \lambda_{\phi_2 \phi_2 \phi_2} &= \lambda_2 s_\beta; \\ \lambda_{\phi_1 AA} &= \lambda_1 c_\beta s_\beta^2 + \frac{\lambda_{34}}{2} c_\beta^3 - \frac{\lambda_5}{2} c_\beta (1 + s_\beta^2), & \lambda_{\phi_2 AA} &= \lambda_2 s_\beta c_\beta^2 + \frac{\lambda_{34}}{2} s_\beta^3 - \frac{\lambda_5}{2} s_\beta (1 + c_\beta^2); \\ \lambda_{\phi_1 G^0 A} &= (-2\lambda_1 + \lambda_{34}) c_\beta^2 s_\beta - \lambda_5 s_\beta^3, & \lambda_{\phi_2 G^0 A} &= (2\lambda_2 - \lambda_{34}) s_\beta^2 c_\beta + \lambda_5 c_\beta^3; \\ \lambda_{\phi_1 G^0 G^0} &= \lambda_1 c_\beta^3 + \frac{\lambda_{345}}{2} c_\beta s_\beta^2, & \lambda_{\phi_2 G^0 G^0} &= \lambda_2 s_\beta^3 + \frac{\lambda_{345}}{2} s_\beta c_\beta^2;\end{aligned}\quad (\text{A8})$$

$$\begin{aligned}\lambda_{\phi_1 G^- G^+} &= 2\lambda_1 c_\beta^3 + \lambda_{345} s_\beta c_\beta^2, & \lambda_{\phi_2 G^- G^+} &= 2\lambda_2 s_\beta^3 + \lambda_{345} c_\beta s_\beta^2, \\ \lambda_{\phi_1 G^\mp G^\pm} &= -2\lambda_1 s_\beta c_\beta^2 + \lambda_3 s_\beta c_\beta^2 + \frac{\lambda_{45}}{2} s_\beta c_2 \beta, & \lambda_{\phi_2 G^\mp G^\pm} &= 2\lambda_2 c_\beta s_\beta^2 - \lambda_3 c_\beta s_\beta^2 + \frac{\lambda_{45}}{2} c_\beta c_2 \beta, \\ \lambda_{\phi_1 H^- H^+} &= 2\lambda_1 c_\beta s_\beta^2 + \lambda_3 c_\beta^3 - \lambda_{45} c_\beta s_\beta^2, & \lambda_{\phi_2 H^- H^+} &= 2\lambda_2 s_\beta c_\beta^2 + \lambda_3 s_\beta^3 - \lambda_{45} s_\beta c_\beta^2,\end{aligned}\quad (\text{A9})$$

with $\lambda_{345} \equiv \lambda_3 + \lambda_4 + \lambda_5$ and $\lambda_{34} \equiv \lambda_3 + \lambda_4$. Notice that $\lambda_{\phi_1 H^+ H^-} = 2\lambda_{\phi_1 AA}$ in the custodial symmetric limit: $\lambda_4 = \lambda_5$.

-
- | | |
|---|--|
| <p>[1] S. R. Coleman and E. J. Weinberg, <i>Phys. Rev. D</i> 7, 1888 (1973).</p> <p>[2] E. Gildener and S. Weinberg, <i>Phys. Rev. D</i> 13, 3333 (1976).</p> <p>[3] R. Barate <i>et al.</i> (ALEPH Collaboration, DELPHI Collaboration, L3 Collaboration, OPAL Collaboration, and LEP Working Group for Higgs Boson Searches), <i>Phys. Lett. B</i> 565, 61 (2003).</p> <p>[4] R. Hempfling, <i>Phys. Lett. B</i> 379, 153 (1996).</p> <p>[5] W.-F. Chang, J. N. Ng, and J. M. S. Wu, <i>Phys. Rev. D</i> 75, 115016 (2007).</p> <p>[6] S. Iso, N. Okada, and Y. Orikasa, <i>Phys. Lett. B</i> 676, 81 (2009).</p> <p>[7] R. Foot, A. Kobakhidze, and R. R. Volkas, <i>Phys. Lett. B</i> 655, 156 (2007).</p> <p>[8] K. A. Meissner and H. Nicolai, <i>Phys. Lett. B</i> 648, 312 (2007); 660, 260 (2008).</p> <p>[9] L. Alexander-Nunneley and A. Pilaftsis, <i>J. High Energy Phys.</i> 09 (2010) 021.</p> | <p>[10] M. Holthausen, M. Lindner, and M. A. Schmidt, <i>Phys. Rev. D</i> 82, 055002 (2010).</p> <p>[11] S. L. Glashow and S. Weinberg, <i>Phys. Rev. D</i> 15, 1958 (1977).</p> <p>[12] M. Shaposhnikov and D. Zenhäusern, <i>Phys. Lett. B</i> 671, 162 (2009).</p> <p>[13] W. D. Goldberger, B. Grinstein, and W. Skiba, <i>Phys. Rev. Lett.</i> 100, 111802 (2008).</p> <p>[14] M. E. Shaposhnikov and F. V. Tkachov, arXiv:0905.4857.</p> <p>[15] G. C. Branco, P. M. Ferreira, L. Lavoura, M. N. Rebelo, M. Sher, and J. P. Silva, <i>Phys. Rep.</i> 516, 1 (2012).</p> <p>[16] N. G. Deshpande and E. Ma, <i>Phys. Rev. D</i> 18, 2574 (1978).</p> <p>[17] A. W. El Kaffas, W. Khater, O. M. Ogreid, and P. Osland, <i>Nucl. Phys.</i> B775, 45 (2007).</p> <p>[18] B. W. Lee, C. Quigg, and H. B. Thacker, <i>Phys. Rev. Lett.</i> 38, 883 (1977).</p> <p>[19] B. W. Lee, C. Quigg, and H. B. Thacker, <i>Phys. Rev. D</i> 16, 1519 (1977).</p> |
|---|--|

- [20] K. Nakamura *et al.* (Particle Data Group), *J. Phys. G* **37**, 075021 (2010).
- [21] S. Schael *et al.* (ALEPH Collaboration, DELPHI Collaboration, L3 Collaboration, and LEP Working Group for Higgs Boson Searches), *Eur. Phys. J. C* **47**, 547 (2006).
- [22] F. Gianotti for the (ATLAS Collaboration), Report No. ATLAS-CONF-2011-163, 2011; CMS Collaboration, Report No. CMS-PAS-HIG-11-032, 2011.
- [23] S. Kanemura, T. Kubota, and E. Takasugi, *Phys. Lett. B* **313**, 155 (1993).
- [24] M. E. Peskin and T. Takeuchi, *Phys. Rev. Lett.* **65**, 964 (1990).
- [25] M. E. Peskin and T. Takeuchi, *Phys. Rev. D* **46**, 381 (1992).
- [26] D. Toussaint, *Phys. Rev. D* **18**, 1626 (1978).
- [27] S. Kanemura, Y. Okada, H. Taniguchi, and K. Tsumura, *Phys. Lett. B* **704**, 303 (2011).
- [28] R. A. Battye, G. D. Brawn, and A. Pilaftsis, *J. High Energy Phys.* **08** (2011) 020.
- [29] A. Pilaftsis, *Phys. Lett. B* **706**, 465 (2012).
- [30] G.-C. Cho and K. Hagiwara, *Nucl. Phys.* **B574**, 623 (2000).
- [31] M. Misiak, H. M. Asatrian, K. Bieri, M. Czakon, A. Czarnecki, T. Ewerth, A. Ferroglia, P. Gambino *et al.*, *Phys. Rev. Lett.* **98**, 022002 (2007).
- [32] R. Foot, A. Kobakhidze, K. L. McDonald, and R. R. Volkas, *Phys. Rev. D* **76**, 075014 (2007).
- [33] K. A. Meissner and H. Nicolai, *Eur. Phys. J. C* **57**, 493 (2008).